



International Journal of Pharmacy & Therapeutics

Journal homepage: www.ijptjournal.com

IJPT

PHARMACOLOGICAL IDENTIFICATION OF ENDOGENOUS SLO1 CHANNEL- β 1 SUBUNIT COMPLEXES IN CHO CELLS USING THREE α KTX1 SUBFAMILY TOXINS

Edgar Garza-López¹, Oscar Sánchez-Carranza¹, Takuya Nishigaki¹,
Ignacio López-González^{1*}

¹Departamento de Genética del Desarrollo y Fisiología Molecular, Instituto de Biotecnología, Universidad Nacional Autónoma de México, Cuernavaca Morelos 62210, México.

ABSTRACT

Although CHO cells are an excellent cellular model for studying the biophysical properties of heterologous expressed voltage-gated K⁺ channels, this cell line has small, but significant, endogenous K⁺ conductances. Here, we show that CHO cells express at least two different endogenous K⁺ currents: the major component was inhibited by the α KTx1 subfamily toxins Charybdotoxin (CbTX), Iberitoxin, and Slotoxin but it was resistant to Clofilium; whereas the minor component was resistant to α KTx1 toxins. Consistently with the pharmacological profile, the current density of the main K⁺ current component was increased in presence of a high internal Ca²⁺ concentration (0.5 mM), suggesting this component is encoded by Slo1 K⁺ channels. The α KTx1 toxins did not affect the activation of the toxin-sensitive K⁺ current, but CbTX slowed the deactivation kinetics. In addition, the sequence of the α KTx1 toxins inhibitory potency suggests that native Slo1 channels are modulated, at least, by endogenous β 1 ancillary subunit. The presence of native β subunits could influence the biophysical properties of heterologously expressed K⁺ channels in this cell line.

Key Words:- Slo1 K⁺ channels; CHO cells; Charybdotoxin; Iberitoxin; Slotoxin; Clofilium.

INTRODUCTION

CHO cell line has constituted an excellent cellular model for studying the biophysical properties and pharmacology of heterologous expressed ion channels. In particular this cell line has been proposed as a good model for the electrophysiological characterization of voltage-gated K⁺ channels due to its low expression level of endogenous K⁺ channels (Di Veroli *et al.*, 2013; Gamper *et al.*, 2005). Interestingly there are few reports regarding the biophysical properties and pharmacology of those CHO cells endogenous K⁺ currents and no information

exists about electrophysiological or pharmacological evidence of their regulatory β subunits. Regarding ionic currents, previous studies have suggested CHO cells express at least four different types of macroscopic ion currents: a Ca²⁺-sensitive K⁺ current; Na⁺ and Ca²⁺ voltage-gated inward currents (Skryma *et al.*, 1994a); and a swelling-activated chloride current (Li *et al.*, 2000). Only the voltage-gated Ca²⁺ current was studied in more detail and it was identified as an L-type Ca²⁺ current based on its pharmacological profile (Skryma *et al.*, 1994b).

Slo1 channels (a.k.a. MaxiK, BK, or KCa1.1) are ubiquitously expressed voltage- and Ca²⁺-activated K⁺ channels of large conductance (>200 pS) (Anderson *et al.*, 1988; Banerjee *et al.*, 2013; MacKinnon and Miller, 1988; Orio *et al.*, 2002). Despite being coded by a single gene

Corresponding Author

Ignacio López-González

Email:- iglogo@ibt.unam.mx

(*kcnma1*), Slo1 channels present a great diversity in their biophysical properties when expressed in different tissues. Channels with different kinetics and Ca^{2+} sensitivity are originated by alternative splicing; however, the most important element producing the differences between splice variants is β -subunit. Slo1 regulatory β -subunits present two transmembrane segments connected by a 120-residue extracellular loop, with cytoplasmic NH_2 - and COOH -terminals.

At present, four β -subunits ($\beta 1$ - $\beta 4$) have been cloned in mammals (Orío *et al.*, 2002). In general, β -subunit increases the stability of the open states and the apparent Ca^{2+} /voltage sensitivity of the α -subunit, also modifies Slo1 channel kinetics and alters its pharmacological properties (Dworetzky *et al.*, 1996; Meera *et al.*, 2000; Orío *et al.*, 2002).

α KTX toxins have proven to be powerful tools for testing the pharmacological, physiological, biophysical and even structural characteristics of K^+ channels. The α KTx1 Charybdotoxin subfamily (Rodríguez de la Vega *et al.*, 2003) are pore-blocking toxins that bind to the extracellular surface of the Slo1 channels with a 1:1 channel:toxin stoichiometry (Anderson *et al.*, 1988; Banerjee *et al.*, 2013). Charybdotoxin (CbTX), Iberiotoxin (IbTX) and Slo toxin (SloTX) are three representative members of the α KTx1 subfamily, their structure contain a triple-stranded β -sheet or a double-stranded β -sheet complemented with a third pseudo-strand at the N-terminal (Rodríguez de la Vega *et al.*, 2003).

Despite this structural homology, the inhibition specificity is characteristic for each toxin; whereas CbTX inhibits Slo1, $\text{K}_v1.2$ and $\text{K}_v1.3$ K^+ channels (Grissmer *et al.*, 1994), IbTX and SloTX are more specific for Slo1 (García-valdes *et al.*, 2001; Meera *et al.*, 2000). As previously mentioned, β subunits can modify the toxin sensitivity of K^+ channels. Considering the differential pharmacological profile related to the presence of a specific β subunit, toxins have been proposed as a pharmacological tools for discriminating specific K^+ channel- β subunit complexes in native tissues (García-valdes *et al.*, 2001; Meera *et al.*, 2000).

Here, we show that CHO cells express at least two different endogenous K^+ currents with distinct pharmacological sensitivity. Consistently with a previous report, the major component of the endogenous CHO cell K^+ current was inhibited by CbTX, IbTX, and SloTX but resistant to clofilium; suggesting this component is encoded by Slo1- $\beta 1$ K^+ channels. The minor component of K^+ currents was insensitive to previous mentioned Slo1 inhibitors.

MATERIALS AND METHODS

Reagents

Charybdotoxin (CbTX), Iberiotoxin (IbTX), and Slo toxin (SloTX) were acquired from Alomone Labs (Jerusalem, Israel). CbTX, IbTX, and SloTX were dissolved in a solution 10 mM HEPES, pH 7; divided into aliquots, and stored frozen until use. Clofilium tosylate (4-Chloro-N,N-diethyl-N-heptylbenzene butanamium tosylate) was purchased from Sigma Aldrich (St. Louis, MO), dissolved in water to make a stock and stored at 4°C . Toxins dilution to the final concentration in the external medium was carried out daily.

Cell culture

CHO cells were maintained in culture using Advanced Dulbecco's modified Eagle's medium (Gibco, Invitrogen) supplemented with 1% antibiotics and 10% bovine fetal serum (Gibco, Life Technologies). Cells were grown in plastic Petri dishes incubated in a humidity-controlled incubator at 37°C and 5% CO_2 (VWR Scientific 2100) up to 80% of confluence.

Electrophysiology

Disaggregated CHO cells were placed on the stage of an inverted microscope (Diaphot 300, Nikon) following 3–4 days in culture, and membrane currents were recorded with an Axopatch 200B amplifier (Molecular Devices, USA) and filtered at 5 kHz (four-pole Bessel filter). Ion currents were digitized respectively using a Digidata 1440A interface (Molecular Devices, USA) and analyzed with the pCLAMP 10.3 and SigmaPlot software suites. Linear capacitative currents were minimized analogically using the capacitative transient cancellation feature of the amplifier. All experiments were carried out at room temperature ($\sim 22^\circ\text{C}$) and the holding potential (HP) was -100 mV. The recording extracellular solution contained (in mM): 160 KMeSO_4 , 1 CaCl_2 , 5 EGTA, 3 MgCl_2 , and 10 N-2-hydroxyethylpiperazine-W-2-ethanesulfonic acid (HEPES). Intracellular solution contained (in mM): 160 KMeSO_4 , 5 EGTA, 3 MgCl_2 , and 10 N-2-hydroxyethylpiperazine-W-2-ethanesulfonic acid (HEPES). The osmolarity of the external and internal solutions was adjusted to 290 or 265 mosmol/kg with sucrose, respectively. In both cases pH was adjusted to 7.3 with KOH. In pharmacological experiments, toxins were added to the bathing solution as indicated in the text. Patch pipettes were made from borosilicate glass and were pulled with a laser micropipette puller P-2000 (Sutter Instruments Co, USA). The typical micropipette electrical resistance was 3–8 M Ω when filled with internal solutions.

Voltage gated K⁺ Currents Recordings

Macroscopic K⁺ currents were acquired in response to 600 ms test pulses of variable amplitude at a sampling frequency of 20 kHz (50 μs). Current to voltage relationships (I–V curves) were obtained by plotting the peak amplitude of ion currents as a function of their respective membrane potential during the test pulse. For the deactivation analysis, data were obtained by fitting a curve to the tail-currents following settling of 95% of the membrane capacitance transient. In all cases, tail-currents were very well fit by a single exponential equation to determine their fast component.

Statistical analysis of data

Statistical analysis was performed using the R 2.11.1 program (The R foundation for statistical computing, 2010). Analysis of variance (ANOVA) and Tukey's test for multiple comparisons were used to compare either the percentages of inhibition of the K⁺ current amplitude of CHO cells, in the absence or presence of different K⁺ channel blockers. Data were expressed as the mean ± standard error of the mean (SEM). A *p* < 0.05 was considered significant. All the experiments were repeated at least three times.

Results

In the present report all electrophysiological recordings were performed on acute disaggregated CHO cells under the whole-cell configuration. Cells had an average capacitance of 32 ± 10 pF (n=17) and input resistances in the range of 3 to 8 GΩ. In our experimental conditions (isotonic K⁺ concentration), CHO cells displayed a family of non-inactivating outward currents when we applied the indicated voltage clamp protocol (Figure 1A, control). The mean current density of endogenous K⁺ currents was ~ 5 ± 2 pA/pF (Figure 1B; n=13).

Outward Rectifier K⁺ Currents in CHO Cells are sensitive to Charybdotoxin, Iberitoxin and SloTxin but Clofilium insensitive

It has been previously reported that Charybdotoxin (CbTX; 30 nM) inhibits around 90% of the voltage-activated K⁺ conductance present in CHO-K1 cells (Skryma *et al.*, 1994a) suggesting this K⁺ current is encoded by Slo1 K⁺ channels. In the present report we assayed two additional Slo1-specific toxins (Iberitoxin and SloTxin) to discard other potential CbTX blocking targets like K_v1.2 or K_v1.3 K⁺ channels (K_d=14 and 2.6 nM, respectively; reported by (Grissmer *et al.*, 1994)). Both K_v1 channels could be present in this cell line according to the CHO-K1 GenBank genome assembly

data (Kcna2 and Kcna3 genes, respectively. GenBank Assembly ID GCA_000223135.1; supplementary table 1). We confirmed that incubating CHO cells in presence of a saturating CbTX concentration (120 nM) inhibited the endogenous K⁺ current by around 80% (Figure 1A, right upper panel; and 1B). This CbTX-sensitive K⁺ current was modulated by the Ca²⁺ concentration of the internal solution. Figure 1C shows that the K⁺ current density of CHO cells increased by 5-fold in presence of Ca²⁺ (0.5 mM) respect to a nominal Ca²⁺ concentration, consistent with the Ca²⁺-dependent open probability of microscopic currents previously reported for this CHO cell K⁺ current (Skryma *et al.*, 1994a). Subtracting the CbTX-resistant component to the whole K⁺ endogenous current of CHO cells revealed the CbTX-sensitive K⁺ current of this cell line (Figure 2A, upper panel and open triangle in I-V curve). Addition of increasing concentrations of CbTX (0.1-200 nM) reduced the K⁺ current amplitude of the CbTX-sensitive component in a dose-dependent manner (Figure 2B). The dose-response curve of CbTX inhibition showed an IC₅₀=31.0 ± 8.8 nM (Figure 2B, opened triangles). Similar results were obtained when Iberitoxin (IbTX) or SloTxin (SloTX) were assayed on the endogenous CHO cells K⁺ current. Addition of IbTX (120 nM) or SloTX (40 nM) reduces 80 or 60 % of the K⁺ current amplitude, respectively (Figure 1A, lower panels; and closed squares and opened diamonds in 1B, respectively). Consistently, the IbTX- or SloTX-sensitive K⁺ current component showed an I-V relationship statistically similar to the previously shown for the CbTX-sensitive component (Figure 2A right panel). The dose-response curve of IbTX inhibition reported an IC₅₀=54.0 ± 6.0 nM (Figure 2B, closed squares). On the other hand, SloTX has been reported as a highly specific toxin against Slo1 channels (Garcia-valdes *et al.*, 2001). Addition of SloTX inhibited the CHO cells K⁺ current with an IC₅₀=29.0 ± 0.2 nM (Figure 2C), showing the highest affinity for this current component. In all cases, the αKTx1 toxins inhibition was voltage-independent in the voltage range from +40 up to +130 mV (Figure 3A). The presence of αKTx1 toxins did not affect the voltage dependency of activation of the K⁺ current (Figure 3B), consistent with the previous description of these toxins as pore blockers rather than gating modifiers (Anderson *et al.*, 1988; Banerjee *et al.*, 2013). An interesting effect was observed regarding the K⁺ current deactivation, only CbTX slowed the deactivation process of the K⁺ current, in particular in a voltage range from +70 up to +130 mV (Figure 3C). Neither IbTX nor SloTX affected the K⁺ current deactivation kinetics.

To discard the potential contribution of Slo3 channel, another Slo K⁺ channel family member present in

the CHO cells genome (Supplementary table 1), to CHO cell macroscopic K^+ currents, we assayed Clofilium (100 μ M) which is a more specific Slo3 inhibitor (Navarro *et al.*, 2007) and does not inhibit Slo1 channels (Fernández-Fernández *et al.*, 2002). Exposing CHO cells to Clofilium did not affect their macroscopic K^+ currents (Figure 3),

indicating that nevertheless the mRNA of Slo3 K^+ channels is present in CHO cell line (supplementary table 1), Slo3 channels are not expressed in these cells or their contribution to the major component of the macroscopic K^+ current is negligible.

Figure 1. The major component of endogenous K^+ currents from CHO cells is modulated by internal Ca^{2+} concentration and it is sensitive to Charybdotoxin (CbTX), Iberiotoxin (IbTX) and Slo toxin (SloTX). A) Representative whole-cell endogenous K^+ currents of CHO cells in response to 600 ms test pulses of 10 mV steps from a holding potential of -100 mV in a voltage range from -80 up to +130 mV in absence (control) or presence of CbTX (120 nM), IbTX (120 nM) or SloTX (80 nM). Insert: peptide sequence comparisons of CbTX, IbTX and SloTX. Cystein residues appear in red. Conserved lysine that putative competes with K^+ appears in green. **B)** Representative current-voltage relationships obtained from the results shown in panel A. CbTX and IbTX (120 nM) inhibited the K^+ current to the same extent, SloTX (80 nM) was a more potent inhibitor. **C)** A high internal Ca^{2+} concentration (0.5 mM; open bar) increased the K^+ current density of the toxin-sensitive component, at +100 mV test pulse, respect to nominal Ca^{2+} (closed bar). Insert: representative traces of evoked current at +100 mV in nominal (lower trace) or high internal Ca^{2+} concentration (0.5 mM; upper trace). Right panel: Ca^{2+} -induced increment in the I-V curve of the CHO cells toxin-sensitive K^+ current (0.5 mM; open circles) compare to nominal Ca^{2+} (closed circles). In all cases symbols or bars represent mean \pm S.E.M. * $p < 0.05$

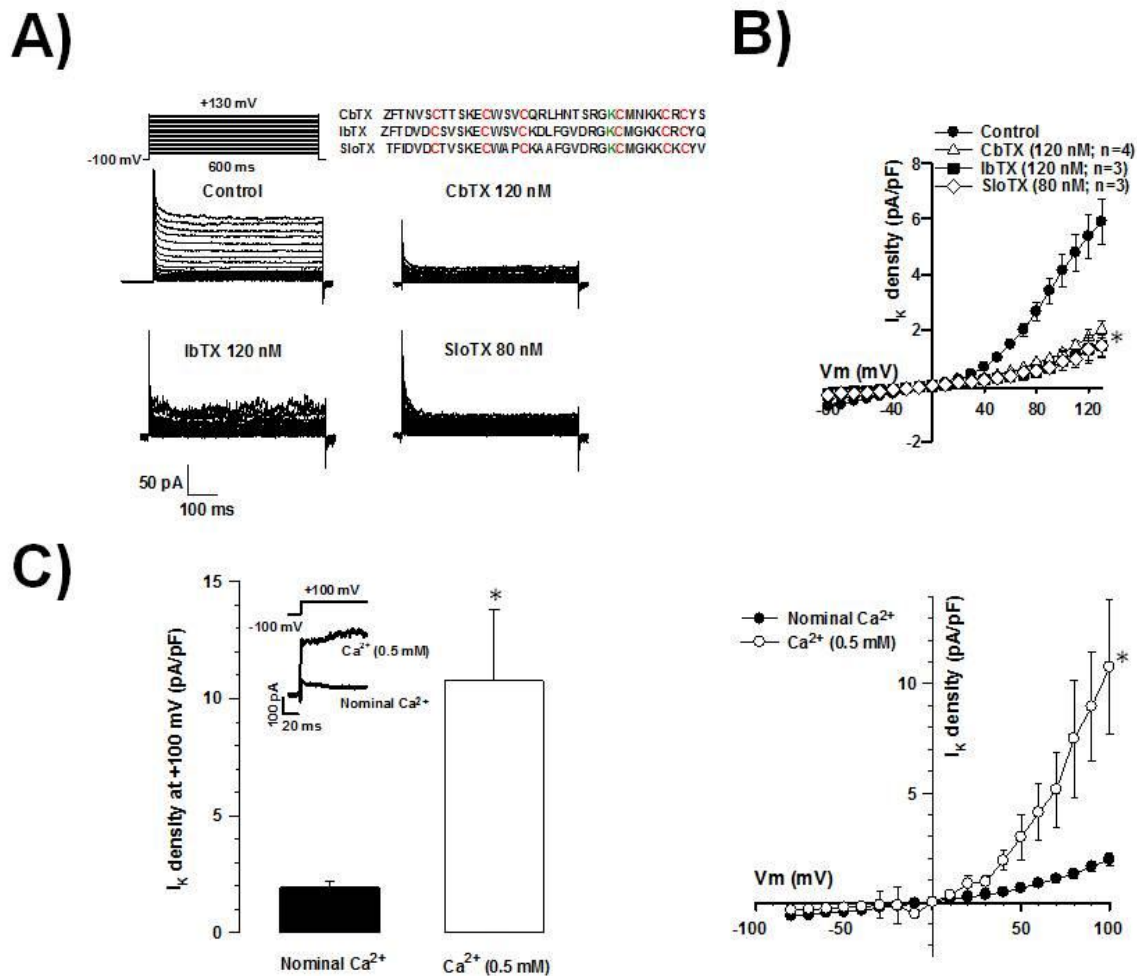


Figure 2. Toxin-sensitive component of the endogenous K⁺ currents showed a pharmacological profile similar to Slo1 channels. A) Representative current families obtained after subtracting experimental recordings treated with CbTX (120 nM), IbTX (120 nM) or SloTX (40 nM) from control recordings. Right panel: corresponding I-V relationships of current families shown in left panel. B) Dose-response curves for CbTX or IbTX inhibition. Following exposure to the indicated concentration of CbTX or IbTX, K⁺ current amplitude evoked with a +130 mV test pulse was normalized to the control at the same voltage. Smooth curves were generated with the Hill equation according to the parameters obtained from the K⁺ currents in each experimental condition (n=3-11). The IC₅₀ for CbTX and IbTX was 31.0 ± 8.8 and 54.0 ± 6.0 nM, respectively. C) CHO cell K⁺ currents were more sensitive to SloTX. Percentage of the K⁺ current inhibition in presence of SloTX (20-80 nM) (n=3-5). In all cases symbols or bars represent mean ± S.E.M.

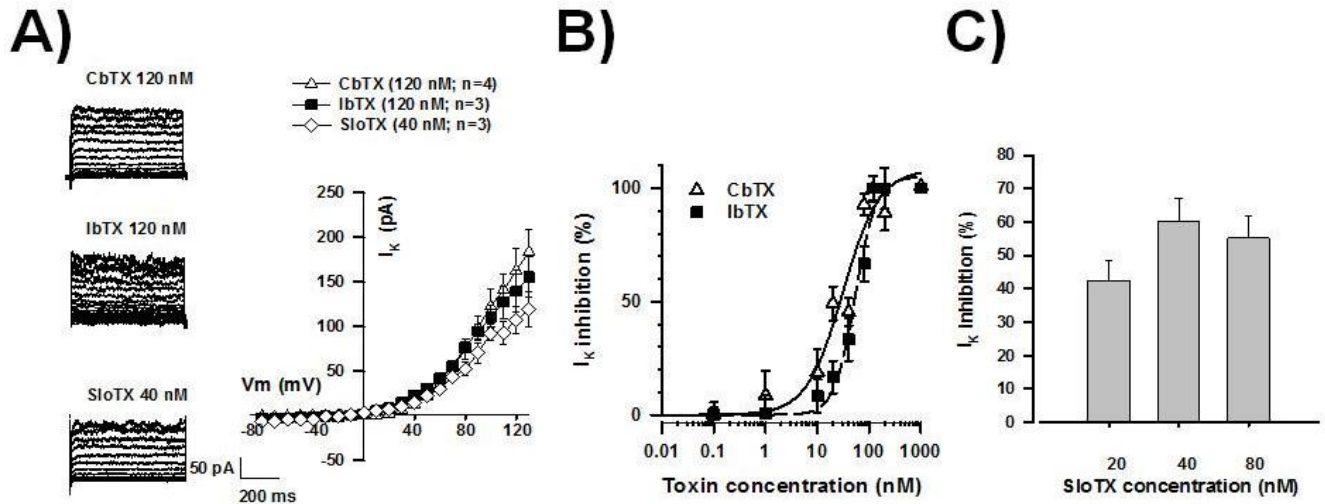


Figure 3. Differential effect of Charybdotoxin subfamily toxins on inhibition, activation and deactivation of the major component of CHO cell K⁺ currents. A) K⁺ current inhibition by α KTx1 toxins was voltage-independent in a depolarized voltage range from +60 up to +130 mV (n=3). B) Addition of α KTx1 toxins does not affect the activation curve of the major component of K⁺ currents. Symbols represent mean ± S.E.M. (n=3-10). C) CbTX (120 nM) was the only α KTx1 subfamily toxin that slowed the deactivation kinetics of endogenous K⁺ currents (n=5). In all cases symbols or bars represent mean ± S.E.M. **p*<0.05

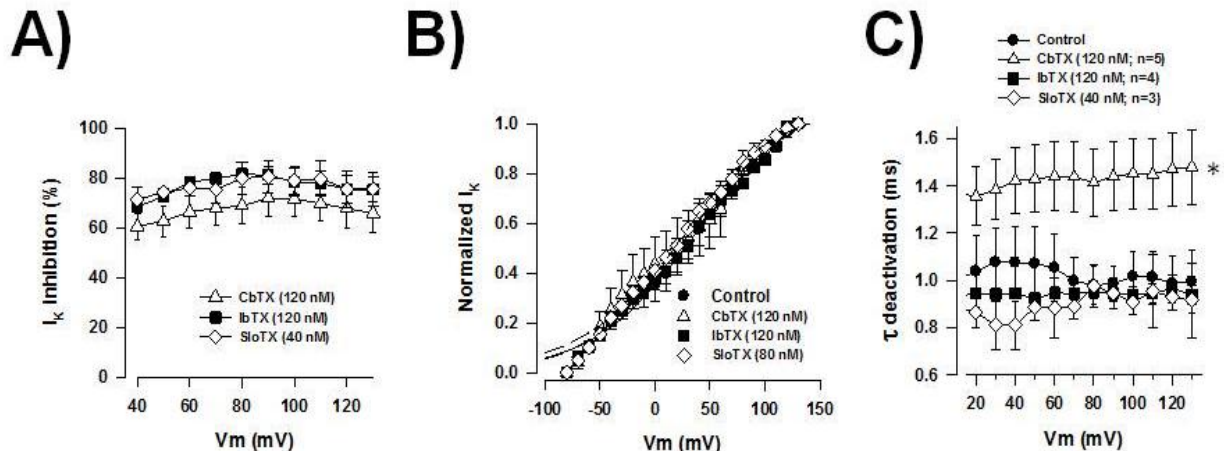
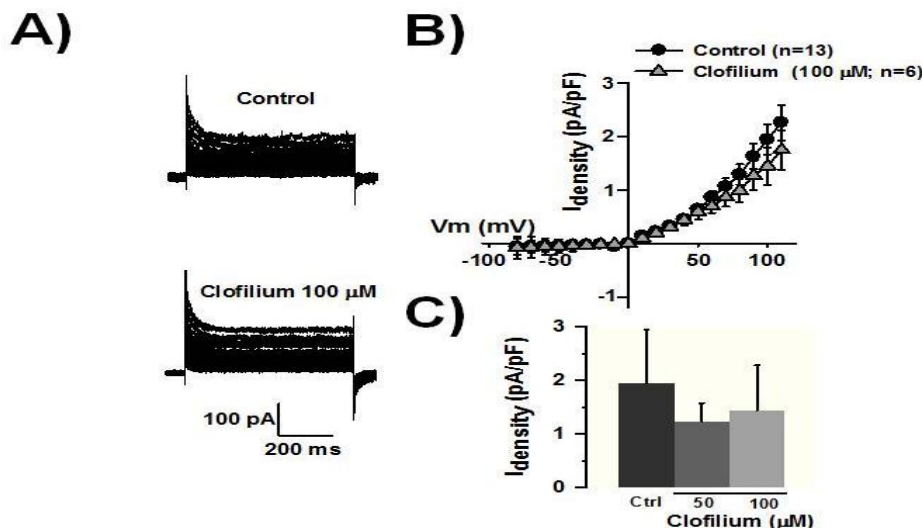


Figure 4. The major component of endogenous K⁺ currents from CHO cells is insensitive to Clofilium, a more specific Slo3 channels inhibitor. **A)** Representative whole-cell K⁺ currents before (upper traces) and after (lower traces) Clofilium addition in external solution (100 μM). **B)** Current-voltage relationships (I-V) in absence (closed circles) or presence (gray triangle) of previously mentioned Clofilium concentration (100 μM). **C)** Two different Clofilium concentrations were assayed on K⁺ current at +100 mV test pulse. K⁺ current density was not affected by the addition of Clofilium (50-100 μM). In all cases symbols or bars represent mean ± S.E.M. (n= 6-13).



DISCUSSION AND CONCLUSION

The pharmacological profile and the Ca²⁺-dependent increasing in the current density of the major component of the CHO cell K⁺ endogenous currents suggest that this αKTx1 toxin-sensitive K⁺ current could be originated by the expression of Slo1 channels. Recent genomic and proteomic data of this cell line support our hypothesis (Baycin-Hizal *et al.*, 2012; Brinkrolf *et al.*, 2013; Hammond *et al.*, 2011; Lewis *et al.*, 2013). The mRNAs for the three Slo channel family members (namely Slo1 (kcnma1), Slo2 (kcnt1 and kcnt2) and Slo3 (kcnu1) channels); and for four different β subunits (β1 (kcmb1), β2 (kcmb2), β3 (kcmb3) and β4 (kcmb4)) are present in CHO cells (from CHO genome, supplementary table 1). Furthermore, proteomic data indicate the protein expression of at least one β1 subunit (KCNAB1) and three different β2 subunit (KCNAB2) isoforms which may interact with K⁺ channels in this cell line (Baycin-Hizal *et al.*, 2012).

Different pharmacological studies have emphasized the β subunit relevance in the large-conductance Ca²⁺- and voltage-activated K⁺ channel sensitivity to toxins (Garcia-valdes *et al.*, 2001; Wu *et al.*, 2012) or intracellular second messengers (Hoshi *et al.*, 2013). In the present report, the CbTX IC₅₀ was 31.0 ± 8.8 nM. Interestingly, the IbTX dose-response curve showed

this toxin exhibited the highest IC₅₀ value (54.0 ± 6.0 nM). Previous reports have shown that the Slo1 inhibition by IbTX could be modified depending on which β ancillary subunit is regulating the α1 subunit. For example, Slo1-β1, -β3 or -β4 coexpression reduces the α1 sensitivity to IbTX even at a high toxin concentration (60, 20 or 80% of current inhibition at 100 nM, respectively) (Dworetzky *et al.*, 1996; Meera *et al.*, 2000; Wu *et al.*, 2012); however the presence of β1 has no effect on the Slo1 inhibition by CbTX (Dworetzky *et al.*, 1996). CbTX (100 nM) completely inhibits Slo1 channels even when they are coexpressed with β1 subunits (100% of current inhibition); however β4 subunit coexpression renders Slo1 channels resistant to the same CbTX concentration (only 20% of current inhibition) (Meera *et al.*, 2000). Considering this information we suggest that in CHO cells Slo1 α subunits could be regulated, at least, by β1 subunits and therefore to be more resistant to IbTX but almost completely inhibited by CbTX (66 and 90% of current inhibition at 100 nM, respectively; Figure 2B). As previously mentioned, the CHO cell line expresses β1, β2, β3 and β4 subunit mRNAs (supplementary table 1 taken from www.chogenome.org); and the CHO proteomic data indicate the presence of, at least, the β1 subunit and three different β2 subunit isoforms in these cells (supplementary table 2 modified from (Baycin-Hizal *et al.*, 2012).

Table 1. K⁺ channels α and β subunits mRNAs present in CHO cells (from Chinese Hamster Genome Database).

Gene name	Access number (GeneBank)	Specification	Synonyms (GeneBank)
Hcn1	100753109	Hyperpolarization Activated Cyclic Nucleotide-Gated Potassium channel 1, transcript variant X1	Human: BCNG1; HAC-2; BCNG-1 Mouse: HAC2; Bcng1; C630013B14Rik
Hcn2	100751563	Hyperpolarization Activated Cyclic Nucleotide-Gated Potassium channel 2, transcript variant X1	Human: BCNG2; HAC-1; BCNG-2 Mouse: BCNG2, HAC1, trls
Hcn3	100772247	Hyperpolarization Activated Cyclic Nucleotide-Gated Potassium channel 3, transcript variant X1	Human: None Mouse: BCNG-4, Bcng4, Hac3, Hcn4
Hcn4	100758754	Hyperpolarization Activated Cyclic Nucleotide-Gated Potassium channel 4, transcript variant X1	Human: SSS2 Mouse: Bcng3, Hcn3
Kcmf1	100753827	Potassium channel modulatory factor 1, transcript variant X4	Human: DEBT91, FIGC, PCMF, ZZZ1 Mouse: 1700094M07Rik, Debt91, Pmcf
Kcnab1	100755538	Potassium Voltage-Gated channel, Shaker-related subfamily, Beta member 1, transcript variant X1	Human: AKR6A3, KCNA1B, KV-BETA-1, Kvb1.3, hKvBeta3, hKvb3 Mouse: Akr8a8, Kvbeta1.1, mKv(beta)1
Kcnab2	100765085	Potassium Voltage-Gated channel, Shaker-related subfamily, Beta member 2, transcript variant X1	Human: RP1-233K16.1, AKR6A5, HKvbeta2, HKvbeta2.1, HKvbeta2.2, KCNA2B, KV-BETA-2 Mouse: RP23-421E12.12-005, F5, I2rf5, Kcnb3, kv-beta-2
Kcnab3	100755337	Potassium Voltage-Gated channel, Shaker-related subfamily, Beta member 3, transcript variant X1	Human: AKR6A9, KCNA3.1B, KCNA3B, KV-BETA-3 Mouse: RP23-26L6.3, C330022D06Rik, Kcnab4, mKv(beta)4
Kcnb1	100759046	Potassium Voltage Gated channel, Shab-related subfamily, member 1	Human: DRK1, KV2.1, h-DRK1 Mouse: RP23-19L12.6, Kcr1-1, Kv2.1, Shab
Kcnb2	100764283	Potassium Voltage Gated channel, Shab-related subfamily, member 2	Human: KV2.2 Mouse: 9630047L19Rik, BB130875, Kv2.2
Kcng1	100758175	Potassium Voltage-Gated channel, subfamily G, member 1	Human: RP5-955M13.1, K13, KCNG, KV6.1, kH2 Mouse: RP23-391M18.5, AW536275, OTTMUSG000000160
Kcng4	100773553	Potassium Voltage-Gated channel, subfamily G, member 4	Human: KV6.3, KV6.4 Mouse: 4921535I01Rik, AW049024, KV6.3, KV6.4
Kcnh1	100764830	Potassium Voltage-Gated channel, subfamily H 8eag-related 9, member 1	Human: EAG, EAG1, Kv10.1, h-eag Mouse: EAG1, Kv10.1, M-eag
Kcnh7	100764883	Potassium Voltage-Gated channel, subfamily H 8eag-related 9, member 7	Human: ERG3, HERG3, Kv11.3 Mouse: RP23-34J8.1, 9330137I11Rik, Kv11.3, erg3
Kcnh8	100773504	Potassium Voltage-Gated channel, subfamily H 8eag-related 9, member 8	Human: ELK, ELK1, Kv12.1, elk3 Mouse: C130090D05Rik, ELK, ELK1, ELK3, Kv12.1
Kcnj1	100766584	Potassium Inwardly-Rectifying channel, subfamily J, member 1	Human: KIR1.1, ROMK, ROMK1 Mouse: Kir1.1, ROMK, Romk2
Kcnj5	100766874	Potassium Inwardly-Rectifying channel, subfamily J,	Human: CIR, GIRK4, KATP1, KIR3.4, LQT13

		member 5	Mouse: GIRK4, Kir3.4
Kcnj10	100764542	Potassium Inwardly-Rectifying channel, subfamily J, member 10	Human: BIRK-10, KCNJ13-PEN, KIR1.2, KIR4.1, SESAME Mouse: BIR10, BIRK-1, Kir1.2, Kir4.1
Kcnj13	100774709	Potassium Inwardly-Rectifying channel, subfamily J, member 13	Human: KIR1.4, KIR7.1, LCA16, SVD Mouse: None
Kcnk1	100762483	Potassium channel, subfamily K, member 1	Human: RP4-550F15.1, DPK, HOHO, K2P1, K2p1.1, KCNO1, TWIK-1, TWIK1 Mouse: AI788889, TWIK-1
Kcnk2	100751502	Potassium channel, subfamily K, member 2, transcript variant X1	Human: K2p2.1, TPKC1, TREK, TREK-1, TREK1, hTREK-1c, hTREK-1e Mouse: A430027H14Rik, AI848635, TREK-1
Kcnk3	100771641	Potassium channel, subfamily K, member 3	Human: K2p3.1, OAT1, PPH4, TASK, TASK-1, TBAK1 Mouse: TASK, Task-1, cTBAK-1
Kcnk4	100760723	Potassium channel, subfamily K, member 4	Human: K2p4.1, TRAAK, TRAAK1 Mouse: MLZ-622, TRAAK, TRAAKt, Tex40
Kcnk5	100760223	Potassium channel, subfamily K, member 5	Human: K2p5.1, TASK-2, TASK2 Mouse: TASK-2
Kcnk6	100764262	Potassium channel, subfamily K, member 6, transcript variant X1	Human: K2p6.1, KCNK8, TOSS, TWIK-2, TWIK2 Mouse: D7Erd764e, Toss, Twik2
Kcnk7	100763826	Potassium channel, subfamily K, member 7	Human: K2p7.1, TWIK3 Mouse: 2310014G03Rik, Kcnk6, Kcnk8, Knot, Mlk3
Kcnk9	100756282	Potassium channel, subfamily K, member 9, transcript variant X1	Human: K2p9.1, KT3.2, TASK-3, TASK3 Mouse: Task3
Kcnk10	100750735	Potassium channel, subfamily K, member 10	Human: K2p10.1, PPP1R97, TREK-2, TREK2 Mouse: 1700024D23Rik, 3010005K24Rik, Trek2
Kcnk12	100770804	Potassium channel, subfamily K, member 12	Human: K2p12.1, THIK-2, THIK2 Mouse: mntk1
Kcnk13	100769761	Potassium channel, subfamily K, member 13	Human: K2p13.1, THIK-1, THIK1 Mouse: BB085247, F730021E22Rik, Gm1570, Gm1685
Kcnk15	100756837	Potassium channel, subfamily K, member 15, transcript variant X1	Human: K2p15.1, KCNK11, KCNK14, KT3.3, TASK-5, TASK5, dJ781B1.1 Mouse: RP23-161B3.2, KCNK11, KCNK14, KT3.3, TASK5
Kcnk16	100760808	Potassium channel, subfamily K, member 16	Human: K2p7.1, TWIK3 Mouse: 2310014G03Rik, Kcnk6, Kcnk8, Knot, Mlk3
Kcnk17	100770528	Potassium channel, subfamily K, member 17, transcript variant X1	Human: UNQ5816/PRO19634, K2p17.1, TALK-2, TALK2, TASK-4, TASK4 Mouse: None
Kcnk18	100774565	Potassium channel, subfamily K, member 18	Human: K2p18.1, MGR13, TRESK, TRESK-2, TRESK2, TRIK Mouse: Gm781, Tresk, Tresk-2, Trik

**Kcnma1	100764731	Potassium Large Conductance Calcium-Activated channel, subfamily M, alpha member 1	Human: RP11-443A13.1, BKTM, KCa1.1, MaxiK, SAKCA, SLO, SLO-ALPHA, SLO1, bA205K10.1 Mouse: RP24-486D21.1, 5730414M22Rik, BKCa, MaxiK, Slo, Slo1, mSlo, mSlo1
*Kcnmb1	100765448	potassium large conductance calcium-activated channel, subfamily M, beta member 1	CaKB; Calcium-activated potassium channel, beta1 subunit.
*Kcnmb2	100761612	potassium large conductance calcium-activated channel, subfamily M, beta member 2	CaKB; Calcium-activated potassium channel, beta2 subunit.
*Kcnmb3	100758210	potassium large conductance calcium-activated channel, subfamily M beta member 3, transcript variant X1, transcript variant X2, transcript variant X3	CaKB; Calcium-activated potassium channel, beta3 subunit.
*Kcnmb4	100754855	potassium large conductance calcium-activated channel, subfamily M, beta member 4, transcript variant X1	CaKB; Calcium-activated potassium channel, beta4 subunit.
Kcnq1	100761481	Potassium Voltage-Gated channel, subfamily Q, member 1	Human: ATFB1, ATFB3, JLNS1, KCNA8, KCNA9, KVLQT1, Kv1.9, Kv7.1, LQT, LQT1, RWS, SQT2, WRS Mouse: AW559127, KVLQT1, Kcna9
Kcnq5	100773342	Potassium Voltage-Gated channel, subfamily Q, member 5	Human: RP11-257K9.5, Kv7.5 Mouse: 7730402H11, 9230107O05Rik, AA589396, D1Mgi1
Kcnrg	100753429	Potassium channel regulator	Human: RP11-34F20.6, DLTET Mouse: C1ld4, E030012H22Rik, Gm745
Kcnt1	100758898	Potassium channel, subfamily T, member 1, transcript variant X1	Human: RP11-100C15.1, EIEE14, ENFL5, KCa4.1, SLACK, bA100C15.2 Mouse: RP23-123F7.3, C030030G16Rik, Slack, mKIAA1422, slo2
Kcnt2	100768557	Potassium channel, subfamily T, member 2, transcript variant X1	Human: RP11-58O13.1, KCa4.2, SLICK, SLO2.1 Mouse: E330038N15Rik, Slick
Kcnu1	100752893	Potassium channel, subfamily U, member 1	Human: KCNMC1, KCa5, KCa5.1, Kcnma3, Slo3 Mouse: Kcnma3, Slo3, mSlo3
Kcnv2	100757476	Potassium channel, subfamily V, member 2	Human: KV11.1, Kv8.2, RCD3B Mouse: KV11.1
Kctd1	100770054	Potassium channel tetramerization domain containing 1, transcript variant X1	Human: hCG_38480, C18orf5, SENS Mouse: 4933402K10Rik, AI661543, AW553000
Kctd2	100757654	potassium channel tetramerization domain containing 2, transcript variant X1	Human: None Mouse: RP23-392H19.1, 2310012I15Rik
Kctd3	100760825	Potassium channel tetramerization domain containing 3, transcript variant X1	Human: RP11-5F19.1, NY-REN-45 Mouse: 4930438A20Rik, 9330185B06, E330032J19Rik, NY-REN-45
Kctd4	100768043	Potassium channel tetramerization domain containing 4	Human: bA321C24.3 Mouse: 2210017A09Rik, AU017169

Kctd5	100772768	Potassium channel tetramerization domain containing 5, transcript variant X1	Human: None Mouse: 2610030N08Rik, mKIAA0176
Kctd6	100765751	Potassium channel tetramerization domain containing 6, transcript variant X1	Human: KCASH3 Mouse: 5430433B02Rik, AU044285
Kctd7	100757850	Potassium channel tetramerization domain containing 7, transcript variant X7	Human: CLN14, EPM3 Mouse: 4932409E18, 9430010P06Rik
Kctd8	100754636	Potassium channel tetramerization domain containing 8, transcript variant X1	Human: None Mouse: A730087N02Rik
Kctd9	100753176	Potassium channel tetramerization domain containing 9, transcript variant X1	Human: BTBD27 Mouse: None
Kctd10	100752520	Potassium channel Tetramerization domain containing 10, transcript variant X1	Human: BTBD28; ULRO61; MSTP028; hBACURD3 Mouse: C87062; AW536343; mBACURD3
Kctd11	100760546	Potassium channel tetramerization domain containing 11	Human: C17orf36, KCASH1, REN, REN/KCTD11 Mouse: RP23-119B10.1, AF465352, Ren
Kctd12	100753862	Potassium channel tetramerization domain containing 12, transcript variant X2	Human: C13orf2, PFET1, PFETIN Mouse: AU046135, AW538430, Pfet1, Pfetin
Kctd13	100753748	Potassium channel tetramerization domain containing 13, transcript variant X1	Human: FKSG86, BACURD1, PDIP1, POLDIP1, hBACURD1 Mouse: 1500003N18Rik, AV259508, PDIP1alpha, P dip1, Poldip1
Kctd14	100768863	Potassium channel tetramerization domain containing 14, transcript variant X1	Human: None Mouse: AI449310, D7Erd760e
Kctd15	100765553	Potassium channel tetramerization domain containing 15, transcript variant X1	Human: None Mouse: RP23-324J22.2, BC031749
Kctd16	100755887	Potassium channel tetramerization domain containing 16	Human: None Mouse: 4930434H12Rik, Gm1267
Kctd17	100763063	Potassium channel tetramerization domain containing 17, transcript variant X2	Human: RP5-1170K4.4 Mouse: 2900008M13Rik, AA414907, AW742389, N28155
Kctd18	100751064	Potassium channel tetramerization domain containing 18, transcript variant X1	Human: 6530404F10Rik Mouse: 4932411A20Rik, 6530404F10Rik
Kctd19	100761191	Potassium channel tetramerization domain containing 19	Human: None Mouse: 4932411A20Rik, 6530404F10Rik
Kctd20	100752436	Potassium channel tetramerization domain containing 20, transcript variant X1	Human: RP1-108K11.2, C6orf69, dJ108K11.3 Mouse: RP24-318I24.4, 2410004N11Rik, AI451943, AW541186, D17Erd562e
Kctd21	100765855	Potassium channel tetramerization domain containing 21, transcript variant X1	Human: KCASH2 Mouse: EG622320

Note: parcial mRNAs present in CHO cells reported by CHO genome database are not included. *mRNAs corresponding to different Slo1 β ancillary subunits.
**mRNA of Slo1 α subunit.

Table 2. Proteomic data of CHO cells show the expression of K⁺ channel β 1 and β 2 subunits (from Chinese Hamster Genome Database).

Protein name	Protein Access ID	Identified Peptide Sequences	Number of Identified Sequences	Number of Identified Spectra	FDR	Coverage	Cluster ID	Group ID	SwissProt Annotation/Homology with Highest Percentage	GO Annotation	KEGG Annotation
Voltage-Gated Potassium Channel subunit beta-2-like isoform 2	gi 354501157 ref XP_003512659.1	ELQAI AER	24	131	0.01013	58	763	4984	KCAB2_RAT: Voltage-Gated Potassium Channel subunit beta-2 OS= <i>Rattus norvegicus</i> GN=Kcnab2 PE=1 SV=1	GO:0016491Oxidoreductase activity; Molecular Function	KCNAB2; Potassium Voltage-Gated Channel, Shaker-related subfamily, beta member 2 K04883 Potassium Voltage-Gated Channel, Shaker-related subfamily A, beta member 2
Voltage-Gated Potassium Channel subunit beta-2-like isoform 3	gi 354501159 ref XP_003512660.1	QTGSP GMIYR	22	129	0	63	763	4985	KCAB2_RAT: Voltage-Gated Potassium Channel subunit beta-2 OS= <i>Rattus norvegicus</i> GN=Kcnab2 PE=1 SV=1	GO:0016491Oxidoreductase activity; Molecular Function	KCNAB2; Potassium Voltage-Gated Channel, Shaker-related subfamily, beta member 2 K04883 Potassium Voltage-Gated Channel, Shaker-related subfamily A, beta member 2
Voltage-Gated Potassium Channel subunit beta-2-like isoform 1	gi 354501155 ref XP_003512658.1	ELQAI AER	24	131	0.01013	63	763	4984	KCAB2_RAT: Voltage-Gated Potassium Channel subunit beta-2 OS= <i>Rattus norvegicus</i> GN=Kcnab2 PE=1 SV=1	GO:0016491Oxidoreductase activity; Molecular Function	KCNAB2; Potassium Voltage-Gated Channel, Shaker-related subfamily, beta member 2 K04883 Potassium Voltage-Gated Channel, Shaker-related subfamily A, beta member 2
Voltage-Gated Potassium Channel subunit beta-1-like	gi 354472456 ref XP_003498455.1	TVAIIR; PDSNT PMEEI VR; EYHLF QREK	8	20	0	16	763	1203	KCAB2_RAT: Voltage-Gated Potassium Channel subunit beta-2 OS= <i>Rattus norvegicus</i> GN=Kcnab2 PE=1 SV=1	GO:0016491Oxidoreductase activity; Molecular Function	KCNAB2; Potassium Voltage-Gated Channel, Shaker-related subfamily, beta member 2 K04883 Potassium Voltage-Gated Channel, Shaker-related subfamily A, beta member 2

Reported in Baycin-Hizal *et al.*, 2012; [20].

The presence of $\beta 1$ subunit in this cell line would be consistent with a stronger K^+ current inhibition by CbTX ($IC_{50} = 31.0 \pm 8.8$ nM) than by IbTX ($IC_{50} = 54.0 \pm 6.0$ nM). Furthermore, in our experimental conditions the toxin-sensitive K^+ current showed no inactivation during the 600 ms test pulses. This biophysical property of a sustained K^+ current in CHO cells discards the potential Slo1- $\beta 2$ or $-\beta 3a,b,c$ isoforms interaction because it is well documented that $\beta 2$ or $\beta 3a,b,c$ subunits induces the inactivation of Slo1 K^+ currents during 200 ms test pulses (Hoshi *et al.*, 2013; Uebele *et al.*, 2000; Wu *et al.*, 2012). This inactivation of the Slo1 K^+ current is caused by the inactivating particle only present in the NH_2 -terminal domain of $\beta 2$ and $\beta 3$ subunits, which can occlude the conduction pathway of both Slo1 and *Shaker* K^+ channels (Orío *et al.*, 2002). Our results are consistent with the aforementioned observations but certainly this hypothesis deserves further investigation.

On the other hand, it has been shown that $\beta 4$ subunit confers complete protection against SloTX to the Slo1 α subunit (0% of current inhibition, (García-valdes *et al.*, 2001)). The highest sensitivity of the endogenous K^+ current to SloTX (60% inhibition at 40 nM, Figure 2C) could be explained as a consequence of the $\beta 4$ absence in the CHO cell line (supplementary table 1), and strongly support a potential modulation of the endogenous Slo1 channels by the native $\beta 1$ subunit, considering that SloTX has been proposed as a pharmacological tool for discriminating α Slo1- $\beta 1$ or $-\beta 4$ complexes in different tissues (García-valdes *et al.*, 2001).

Regarding CbTX, this toxin shows a considerable diversity of effects on the biophysical properties of different K^+ channels (Sprunger *et al.*, 1996). Whereas a CbTX voltage-dependent inhibition was described for single Ca^{2+} -activated K^+ channel from rat muscle in planar lipid bilayers (Anderson *et al.*, 1988; MacKinnon and Miller, 1988); the CbTX inhibition was voltage-independent on CbTX-sensitive K^+ currents from rat alveolar epithelial cells (Jacobs and Decoursey, 1990) or on heterologous expressed $K_v1.2$ K^+ channels (Sprunger *et al.*, 1996). According to our results, all $\alpha KTx1$ subfamily toxins showed a voltage-independent inhibition (Figure 3A) in the assayed voltage range (from +40 up to +130 mV), suggesting that $\alpha KTx1$ toxins bind to partial or totally activated Slo1 channels at the same extent. As previously mentioned, none of the $\alpha KTx1$ toxins affected the activation curve (Figure 3B), consistent with the previous description of these toxins as pore blockers rather than gating modifiers. Interestingly CbTX increased the deactivation constant of CHO cells K^+ currents (Figure 3C). Previous reports indicate that the CbTX-induced variations in the deactivation kinetics of K^+ channels may

reflect changes in one or more open to closed transition rate constants in addition to blocking the pore (Sprunger *et al.*, 1996). Our results suggest that after repolarization, CbTX reduces the channel returning to the closed state increasing precisely the deactivation constant but IbTX or SloTX do not.

There is a residual component which should be characterized in the future. Skryma and collaborators (1994) (Skryma *et al.*, 1994a) reported that CbTX 30 nM almost completely inhibited the macroscopic K^+ current in CHO cells. These data differ from our observations. Unfortunately we were unable to compare our results with those of the previous report because the CbTX effect on the macroscopic K^+ currents was not shown; and only one CbTX concentration was assayed (Skryma *et al.*, 1994a).

As previously mentioned, CHO cells are an excellent expression system to characterize the pharmacology of heterologous K^+ channels. However, the influence of CHO cell endogenous K^+ current on pharmacological assays could be important in cases where the expression level of heterologous K^+ channels is low to clearly distinguish the expressed heterologous target, as reported for Slo3 K^+ channels expressed in this cell line (Brenker *et al.*, 2014; López-González *et al.*, 2014).

In conclusion, the pharmacological profile presented by the main component of the endogenous K^+ current in this cell line is consistent with the reported pharmacology for Slo1 K^+ channels, which could be associated to, at least, $\beta 1$ ancillary subunit.

ACKNOWLEDGEMENTS

The authors thank Jose Luis De la Vega, Yoloxóchitl Sánchez, Shirley Ainsworth, and Elizabeth Mata for technical assistance. We thank Juan Manuel Hurtado, Roberto Rodríguez, and Arturo Ocádiz for computer services. This work was supported by Consejo Nacional de Ciencia y Tecnología (CONACyT-Mexico) (177138 to TN, and 84362 to ILG); Dirección General de Asuntos del Personal Académico/ Universidad Nacional Autónoma de México (DGAPA/ UNAM) (IN203513 to TN and IN204914 to ILG). Additionally EGL and OSC were recipients of a (DGAPA/UNAM) postdoctoral fellowship and a CONACyT graduate fellowship, respectively.

Conflict of interest statement

The authors declare that there are no conflicts of interest.

Authors' contribution to the study

EGL, OSC, and ILG contributed substantially to the acquisition and analysis of data; drafting the article

and final approval of the version to be published. ILG and TN substantially contributed to the study design, critically

reviewing the article for intellectual content and final approval of the version to be published.

REFERENCES

- Anderson CS, Mackinnon R, Smith C. Charybdotoxin Block of Single Ca²⁺-activated K⁺ channels Effects of Channel Gating, Voltage, and Ionic Strength. *J Gen Physiol*, 91, 1988, 317–333.
- Banerjee A, Lee A, Campbell E, Mackinnon R. Structure of a pore-blocking toxin in complex with a eukaryotic voltage-dependent K(+) channel. *Elife*, 2, 2013, e00594.
- Baycin-Hizal D, Tabb DL, Chaerkady R, Chen L, Lewis NE, Nagarajan H, Sarkaria V, Kumar A, Wolozny D, Colao J, Jacobson E, Tian Y, O’Meally RN, Krag SS, Cole RN, Palsson BO, Zhang H, Betenbaugh M. Proteomic analysis of Chinese hamster ovary cells. *J Proteome Res*, 11, 2012, 5265–76.
- Brenker C, Zhou Y, Müller A, Echeverry FA, Trötschel C, Poetsch A, Xia, X, Bönigk, W, Lingle CJ, Kaupp UB, Strücker T. The Ca²⁺-activated K⁺ current of human sperm is mediated by Slo3. *Elife*, e01438, 2014, 1–19.
- Brinkrolf K, Rupp O, Laux H, Kollin F, Ernst W, Linke B, Kofler R, Romand S, Hesse F, Budach WE, Galosy S, Müller D, Noll T, Wienberg J, Jostock T, Leonard M, Grillari J, Tauch A, Goesmann A, Helk B, Mott JE, Pühler A, Borth N. Chinese hamster genome sequenced from sorted chromosomes. *Nat Biotechnol*, 31, 2013, 694–5.
- Chinese Hamster Genome Database. URL:www.chogenome.org. Last update: May 8, 2014. Last access: October 24, 2014.
- Di Veroli GY, Davies MR, Zhang H, Abi-Gerges N, Boyett MR. High-throughput screening of drug-binding dynamics to HERG improves early drug safety assessment. *Am J Physiol Heart Circ Physiol*, 304, 2013, H104–17.
- Dworetzky SI, Boissard CG, Lum-Ragan JT, McKay MC, Post-Munson DJ, Trojnacki JT, Chang CP, Gribkoff VK. Phenotypic alteration of a human BK (hSlo) channel by hSlobeta subunit coexpression: changes in blocker sensitivity, activation/relaxation and inactivation kinetics, and protein kinase A modulation. *J Neurosci*, 16, 1996, 4543–50.
- Fernández-Fernández JM, Nobles M, Currid A, Vázquez E, Valverde MA. Maxi K⁺ channel mediates regulatory volume decrease response in a human bronchial epithelial cell line. *Am J Physiol Cell Physiol*, 283, 2002, C1705–14.
- Gamper N, Stockand JD, Shapiro MS. The use of Chinese hamster ovary (CHO) cells in the study of ion channels. *J Pharmacol Toxicol Methods*, 51, 2005, 177–85.
- García-valdes J, Zamudio FZ, Toro L, Possani LD. Slotoxin, alpha KTx1.11, a new scorpion peptide blocker of MaxiK channels that differentiates between alpha and alpha + beta (beta1 or beta4) complexes. *FEBS Lett*, 505, 2001, 369–373.
- Grissmer S, Nguyen AN, Aiyar J, Hanson DC, Mather RJ, Gutman GA, Karmilowicz MJ, Auperin DD, George Chandy K. Pharmacological Characterization of Five Cloned Voltage-Gated Expressed in Mammalian Cell Lines. *Mol Pharmacol*, 45, 1994, 1227–1234.
- Hammond S, Swanberg JC, Kaplarevic M, Lee KH. Genomic sequencing and analysis of a Chinese hamster ovary cell line using Illumina sequencing technology. *BMC Genomics*, 12, 2011, 67.
- Hoshi T, Tian Y, Xu R, Heinemann SH, Hou S. Mechanism of the modulation of BK potassium channel complexes with different auxiliary subunit compositions by the omega-3 fatty acid DHA. *Proc Natl Acad Sci U.S.A*, 110, 2013, 4822–7.
- Jacobs A, Decoursey E. Mechanisms of Potassium Channel Block in Rat Alveolar. *J Pharmacol Exp Ther*, 255, 1990, 459–472.
- Lewis NE, Liu X, Li Y, Nagarajan H, Yerganian G, O’Brien E, Bordbar A, Roth AM, Rosenbloom J, Bian C, Xie M, Chen W, Li N, Baycin-Hizal D, Latif H, Forster J, Betenbaugh MJ, Famili I, Xu X, Wang J, Palsson BO. Genomic landscapes of Chinese hamster ovary cell lines as revealed by the *Cricetulus griseus* draft genome. *Nat Biotechnol*, 31, 2013, 759–65.
- Li X, Shimada K, Showalter L a Weinman S a. Biophysical properties of ClC-3 differentiate it from swelling-activated chloride channels in Chinese hamster ovary-K1 cells. *J Biol Chem*, 275, 2000, 35994–8.
- López-González I, Torres-Rodríguez P, Sánchez-Carranza O, Solís-López a Santi CM, Darszon a Treviño CL. Membrane hyperpolarization during human sperm capacitation. *Mol Hum Reprod*, 20, 2014, 619–29.
- MacKinnon R, Miller C. Mechanism of Charybdotoxin Block of the high-conductance, Ca²⁺-activated K⁺ channel. *J Gen Physiol*, 91, 1988, 335–349.
- Meera P, Wallner M, Toro L. A neuronal beta subunit (KCNMB4) makes the large conductance, voltage- and Ca²⁺-activated K⁺ channel resistant to charybdotoxin and iberiotoxin. *Proc Natl Acad Sci U.S.A*, 97, 2000, 5562–7.

- Navarro B, Kirichok Y, Clapham DE. KSper, a pH-sensitive K⁺ current that controls sperm membrane potential. *Proc Natl Acad Sci U.S.A.*, 104, 2007, 7688–7692.
- Orio P, Rojas P, Ferreira G, Latorre R. New Disguises for an Old Channel : MaxiK Channel-Subunits. *Physiology*, 17, 2002,156–161.
- Rodríguez de la Vega RC, Merino E, Becerril B, Possani LD. Novel interactions between K⁺ channels and scorpion toxins. *Trends Pharmacol Sci*, 24, 2003, 222–7.
- Skryma R, Prevarskaya N, Vacher P, Dufy B. Voltage-dependent ionic conductances in Chinese hamster ovary cells. *Am J Physiol Cell Physiol*, 267, 1994a, C544–C553.
- Skryma R, Prevarskaya N, Vacher P, Dufy B. Voltage-dependent Ca²⁺ channels in Chinese hamster ovary (CHO) cells. *FEBS Lett*, 349, 1994b, 289–94.
- Sprunger LK, Stewig NJ, Grady SMO. Effects of charybdotoxin on K⁺ channel (Kv 1.2) deactivation and inactivation kinetics. *Eur J Pharmacol*, 314, 1996, 357–364.
- Uebele VN, Lagrutta a Wade T, Figueroa DJ, Liu Y, McKenna E, Austin CP, Bennett PB, Swanson R. Cloning and functional expression of two families of beta-subunits of the large conductance calcium-activated K⁺ channel. *J Biol Chem*, 275, 2000, 23211–8.
- Wu RS, Liu G, Zakharov SI, Chudasama N, Motoike H, Karlin A, Marx SO. Positions of β 2 and β 3 subunits in the large-conductance calcium- and voltage-activated BK potassium channel. *J Gen Physiol*, 141, 2012, 105–17.